

Antiferromagnetic alignment and relaxation rate of Gd spins in the high temperature superconductor $\text{GdBa}_2\text{Cu}_3\text{O}_{7-\delta}$

R. J. Ormeno and C. E. Gough

School of Physics and Astronomy, The University of Birmingham, Edgbaston, Birmingham, B15 2TT, United Kingdom

Guang Yang

Department of Metallurgy and Materials, The University of Birmingham, Birmingham, B15 2TT, United Kingdom

(Received 12 January 2000; published 20 February 2001)

The complex surface impedance of a number of $\text{GdBa}_2\text{Cu}_3\text{O}_{7-\delta}$ single crystals has been measured at 10, 15, and 21 GHz using a cavity perturbation technique. At low temperatures a marked increase in the effective penetration depth and surface resistance is observed associated with a frequency dependent paramagnetic and antiferromagnetic alignment of the Gd spins. The effective penetration depth has a sharp change in slope at the Néel temperature, $T_N \sim 2.2$ K, with a peak in the surface resistance slightly above. The observed temperature and frequency dependence can be described by a model which assumes a negligibly small interaction between the Gd spins and the electrons in the superconducting state, with a frequency dependent magnetic susceptibility and a Gd spin relaxation time τ_s being a strong function of temperature. Above T_N , τ_s has a component varying as $1/(T-T_N)$, while below T_N it increases $\sim T^{-5}$.

DOI: 10.1103/PhysRevB.63.104517

PACS number(s): 74.25.Ha, 74.25.Nf, 74.72.Jt

One of the surprising early discoveries about high-temperature superconductors was their apparent insensitivity to out-of-plane magnetic ions, with the superconducting properties of $\text{YBa}_2\text{Cu}_3\text{O}_{7-\delta}$ (YBCO) remaining almost unchanged when yttrium was replaced by magnetic rare-earth ions, with the exception of Ce, Pr, and Tb.¹ Furthermore, the low-temperature antiferromagnetic properties were observed to be independent of doping. The thermodynamic superconducting and antiferromagnetic properties of $\text{GdBa}_2\text{Cu}_3\text{O}_{7-\delta}$ (GBCO) therefore appear to be completely uncoupled.^{2,3} However, there remains the possibility that the mutual interaction of the rare-earth (RE) spins and the superconducting electrons could lead to changes in their dynamic properties. Interest in the antiferromagnetic alignment of the rare-earth spins has also re-emerged as a likely explanation of the anomalous increase in the microwave surface resistance of GBCO thin films observed at low temperatures.⁴⁻⁶

We have therefore undertaken a systematic microwave investigation of the antiferromagnetic spin alignment in a number of GBCO single crystals. The surface impedance has been measured to well below the Gd Néel temperature $T_N \sim 2.2$ K, using a hollow dielectric resonator technique.⁷ Measurements at 10, 15, and 21 GHz confirm the influence on microwave properties of the alignment of the Gd spins and enable us to determine the Gd spin relaxation time τ_s both above and below the Néel temperature.

In the superconducting state the microwave surface impedance is given by

$$Z_s = \sqrt{\frac{i\mu_r\mu_0\omega}{(\sigma_1 - i\sigma_2)}} = R_s + iX_s, \quad (1)$$

where σ_1 is the normal-state quasiparticle conductance $n_{qp}e^2\tau_{qp}/m$ (τ_{qp} is the quasiparticle scattering time), R_s is the surface resistance, and X_s is the surface reactance. In the ideal superconducting state $\sigma_2(T) = n_s(T)e^2/m\omega = (\lambda(T)^2\mu_0\omega)^{-1}$, where $\lambda(T)$ is the penetration depth un-

perturbed by any coexistent magnetic properties. An effective permeability for a rate dependent magnetic spin alignment is assumed of the form $\mu_r(T, \omega) = 1 + \chi(T)/[1 + i\omega\tau_s(T)]$, with a spin lattice relaxation time τ_s . For an antiferromagnetic system above the Néel temperature T_N we expect $\chi(T) = C/(T + T_N)$, with $C = n\mu_B^2 p^2/12\pi k_B$, where n is the number of spins per unit volume. DC magnetic measurements give an effective moment $p = 7.82$,⁸ in good agreement with the free ion value of 7.92. Rewriting Z_s as $[i\mu_0\omega/\sigma_{eff}]^{1/2}$, we can define an effective conductivity as

$$\sigma_{eff} = \frac{(\sigma_1 - i\sigma_2)}{1 + \chi/(1 + i\omega\tau_s)}. \quad (2)$$

The real and imaginary parts are give by

$$\sigma_{1eff} = \frac{(1 + \omega^2\tau_s^2)(\Gamma\sigma_1 + \sigma_2\chi\omega\tau_s)}{\Gamma^2 + \chi^2\omega^2\tau_s^2} \quad (3)$$

and

$$\sigma_{2eff} = \frac{(1 + \omega^2\tau_s^2)(\sigma_1\chi\omega\tau_s - \Gamma\sigma_2)}{\Gamma^2 + \chi^2\omega^2\tau_s^2}, \quad (4)$$

where $\Gamma = 1 + \omega^2\tau_s^2 + \chi$. At low temperature, we will show that $\omega\tau_s > 1$, so that

$$\sigma_{1eff}^{approx} \sim \sigma_1 + \sigma_2\chi/\omega\tau_s \quad (5)$$

and

$$\sigma_{2eff}^{approx} \sim \sigma_2(1 + \chi/\omega^2\tau_s^2 + 2/\omega^2\tau_s^2) - \sigma_1\chi/\omega\tau_s, \quad (6)$$

where we retained terms to second order in $1/\omega\tau_s$ because $\sigma_2 \gg \sigma_1$. The usual expressions for $R_s = 1/2\omega^2\mu_0^2\sigma_{1eff}\lambda^3$ and $X_s = (\omega\mu_0/\sigma_{2eff})^{1/2} = \omega\mu_0\lambda_{eff}$ can then be used to extract the real and imaginary parts of the effective conductivity,

with the assumptions that $\sigma_{1eff} \ll \sigma_{2eff}$ and λ represents the London penetration depth unperturbed by the coexistent magnetism.

In fitting our data we have also assumed no change in the quasiparticle conductance from the Gd spin fluctuations. To test the validity of this model, we have measured the surface impedance of several GBCO single crystals both above and below T_N and at several microwave frequencies.

The GBCO crystals were grown in BaZrO_3 crucibles to minimize contamination.^{9,10} The largest crystal used in these measurements was $1.0 \times 1.1 \times 0.06 \text{ mm}^3$ with a T_c of 93 K. During the course of the experiments, with the sample held overnight at room temperature under vacuum, the microwave transition at T_c was observed to broaden, with a second transition emerging at ~ 63 K. This second transition is similar to earlier measurements by Srikanth *et al.* on a similarly grown YBCO crystal, which was interpreted as a second energy gap¹¹. We believe the anomaly is more likely to be associated with oxygen diffusion out of the sample, resulting in surface regions of oxygen deficient, 60 K phase. This may be a generic problem for BaZrO_3 -grown high-temperature superconducting crystals held in vacuum at room temperature for any length in time. However, no associated changes were observed in the low-temperature microwave properties in our measurements.

The surface impedance was measured using a cylindrical dielectric resonator with a 2 mm hole passing along its axis. The resonator was placed centrally within an oxygen-free high-conductivity copper cavity. Measurements were made using the TE_{01n} resonant modes with a typical unloaded Q values of $\sim 10^5$ at 10 GHz. The measurements were undertaken at low microwave power with an average microwave field strength of $\sim \mu\text{T}$. The temperature of the dielectric resonator and copper cavity was held constant at the helium bath temperature. The sample was placed at a magnetic-field antinode of the dielectric resonator, and was supported on the end of a long sapphire rod passing centrally through the resonator. The crystal could be heated from 1.2 K to well above T_c by a heater mounted outside the cavity. Experiments were performed with the c axis parallel or perpendicular to the rf magnetic field, to investigate the effect of magnetic anisotropy. From neutron-diffraction experiments, the Gd spins are known to align along the c axis.³ Measurements were made at three of the resonant modes of the dielectric resonator close to 10, 15, and 21 GHz with suitable positioning of the sample.

The microwave properties were determined by a conventional cavity perturbation method using a Hewlett Packard 8722C Network analyzer with additional data processing to obtain accurate measurements of the resonant frequency f_0 and half power bandwidth f_B of the dielectric cavity resonances. The changes in these values with temperature can be related to the surface impedance by the cavity perturbation formula, $\Delta f_B(T) - 2i\Delta f_0(T) = \Gamma(R_s + i\Delta X_s)$. The resonator constant Γ was determined from measurements with the sample replaced by a chemically polished niobium sample of the same size and known resistivity. We were able to achieve a measurement accuracy and reproducibility for R_s of $\pm 20 \mu\Omega$ and an error in $\Delta\lambda = \pm 0.3 \text{ \AA}$, for a sample of area $0.5 \times 1.1 \text{ mm}^2$ at 10 GHz.

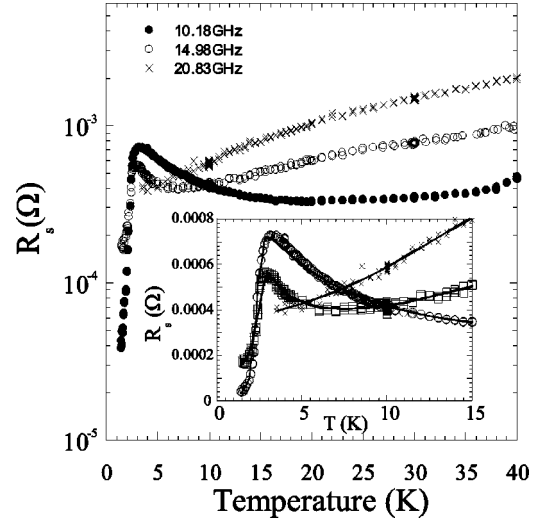


FIG. 1. The surface resistance $R_s(T)$ for currents flowing in the $a-b$ plane of a high-quality $\text{GdBa}_2\text{Cu}_3\text{O}_{7-\delta}$ single crystal. The inset shows an expanded view of the low-temperature region. The solid lines represent calculated values of $R_s(T)$ using Eqs. (3) and (7), with values of $\chi(T)$ and τ_s derived from our model.

Figure 1 shows measurements of $R_s(T)$ at the three frequencies. For $T \geq 30$ K the losses are quadratic in ω , consistent with $\omega\tau_{qp} \ll 1$. In absolute terms, the losses are somewhat larger than observed in the best YBCO crystals, but are comparable with R_s data for near optimally doped $\text{Bi}_2\text{Sr}_2\text{CaCu}_2\text{O}_{8+\delta}$ crystals.^{6,12} At lower temperatures there is a marked and strongly frequency dependent rise in losses, which we associate with the paramagnetic alignment of the Gd spins above the Néel temperature. The losses at 10 GHz peak at 3.5 K, significantly above the Néel temperature of 2.2 K (see inset of Fig. 1). These losses then decrease by more than an order of magnitude at the lowest temperatures.

The spin alignment also leads to a small but pronounced increase in the reactive part of the surface impedance at low temperatures, as shown for two frequencies in Fig. 2. This corresponds to an increased penetration depth with a sharp change in slope defining the Néel temperature. Above ~ 7 K, the reactance increases as $\sim T^2$, in contrast to the T dependence observed for high quality YBCO crystals. The magnitude of these losses and the T^2 dependence of the penetration depth imply a larger quasiparticle scattering than observed in optimally doped YBCO crystals.¹³ Above 10 K we have the expected ω dependence of X_s , but at low temperatures ($T < 7$ K) the reactance has a ω^{-1} dependence, as predicted by our model. The inset illustrates measurements with the crystal aligned with its c axis parallel and perpendicular to the microwave magnetic field (open and closed circles, respectively). In a parallel microwave field, the expected direction of spin alignment, the reactance drops linearly below a well-defined transition temperature $T_N \sim 2.25$ K, but in the perpendicular configuration the susceptibility below T_N is much flatter and may even go through a small maximum. Similar results to those illustrated in Figs. 1 and 2 were observed for all three single crystals investigated. The crystals included slightly underdoped, as-grown and close to optimum-doped oxygen annealed samples, from different growth batches.

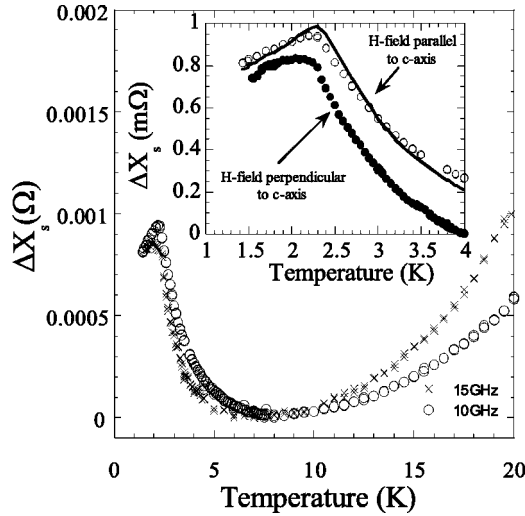


FIG. 2. The surface reactance at 10 and 15 GHz with the \mathbf{H} field parallel to the c -axis. The inset shows $\Delta X_s(T)$ for two crystal orientations at 10 GHz, the solid line represents a fit using Eq. (4) and $X_s = (\omega \mu_0 / \sigma_{2eff})^{1/2}$. Open circles are for the \mathbf{H} field parallel to the c axis and the closed circles for the field perpendicular to the c axis.

To extract an effective conductivity σ_{1eff} from

$$R_s = \frac{1}{2} \omega^2 \mu_0^2 \sigma_{1eff} \lambda^3, \quad (7)$$

we have assumed: (i) a value for $\lambda(0) = 140$ nm, typical of high-quality YBCO samples, (ii) above 10 K, there is no magnetic contribution to $X_s = \mu_0 \omega \lambda$ so that $\sigma_{2eff} \sim \sigma_2$, and (iii) below 10 K, we have extrapolated σ_2 consistent with the T^2 temperature dependence of $X_s(T)$ in Fig. 2. We have also assumed that σ_1 is not significantly affected by the Gd spin fluctuations. Figure 3 shows the temperature dependence of the derived values of σ_{1eff} for all three frequencies measured. Because the contribution to the effective conductivity from the Gd spins varies $\sim 1/\omega \tau_s$, using the 10 and 15 GHz

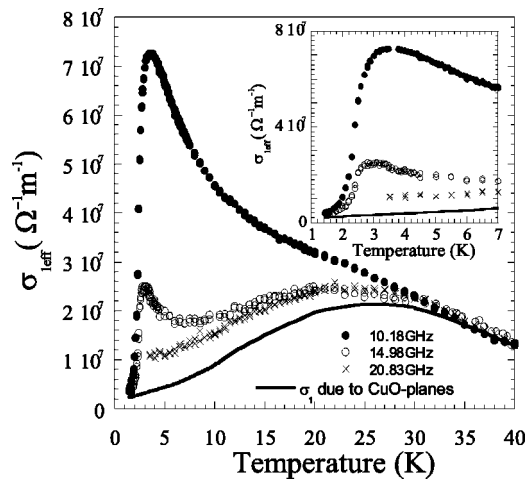


FIG. 3. The temperature dependence of real part of the microwave conductivity extracted from the data in Fig. 1. The solid curve is $\sigma_1(T)$ due to the Cu-O planes. The inset is an expanded view of the low-temperature behavior.

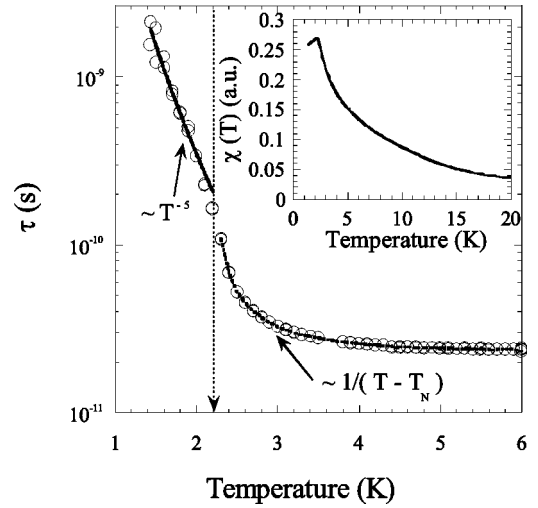


FIG. 4. The temperature dependence of the spin lattice relaxation time extracted from the 10 GHz data. At the Néel temperature there is an apparent change in slope in $\tau_s(T)$. Above T_N , $\tau_s(T) \sim [T_N/(T - T_N)]^\alpha$ with the best fit obtained for $\alpha = 1$, below T_N the relaxation time varies as $\sim T^{-5}$. The inset demonstrates the temperature dependence of χ used to extract $\tau_s(T)$.

data and Eq. 5, we can extract σ_1 giving the solid line. The derived temperature dependence is similar to the variation of $\sigma_1(T)$ observed in YBCO single crystals. It increases to a broad peak at about 25 K, reflecting the increase in the quasiparticle scattering lifetime at low temperatures.

In our model, the additional losses when $\omega \tau_s > 1$ are largely associated with the paramagnetic relaxation of the Gd spins in the microwave field. These losses, which we interpret as a decrease in the Gd spin relaxation rate on approaching and passing through the antiferromagnetic phase transition, peak at a frequency dependent temperature significantly above T_N . In this respect, we note that there is no significant change in σ_{1eff} at the Néel temperature T_N (see inset of Fig. 3). Any such affect is masked by the much larger changes in τ_s , Fig. 4 which has been evaluated using Eq. 5.

The region near T_N might be expected to be dominated by antiferromagnetic spin fluctuations. We assume that close to T_N , τ_s involves a temperature-dependent term varying as $[T_N/(T - T_N)]^\alpha$. A fit to this relation for $\alpha = 1$ is shown in Fig. 4. Below the antiferromagnetic transition τ_s increases by an order of magnitude varying $\sim T^{-5}$ with an apparent change in slope at T_N . The inset of Fig. 4 shows $\chi(T)$ used to derive the temperature dependence of τ_s . This assumes a Curie-Weiss temperature dependence above T_N and a slight drop in $\chi(T)$ below T_N consistent with the measurement shown in the inset of Fig. 2.

The model we have applied assumes that there is no interaction between the quasiparticles and spins (this is consistent with specific heat data on GBCO where no change is observed between semiconducting and superconducting samples²). Susceptibility measurements on nonsuperconducting GBCO have shown that $\chi(T)$ fits a two-dimensional (2D) Ising model above T_N .¹⁴ Below the transition $\chi(T)$ remains anomalously high, deviating from the Ising model.

This is consistent with our reactance measurements, where we see only a small change in $\Delta X_s(T)$ below T_N , Fig. 2. This is in contrast to what is seen in other RE substitutions (Sm, Dy, and Nd) where the specific heat data can be fitted to a 2D Ising model both above and below T_N .¹⁵

In the insets of Figs. 1 and 2, the solid lines fitted to the data have been evaluated using Eqs. (3) and (4) with the usual expressions for R_s and X_s . We have assumed: (i) $\chi(T) = C/(T + T_N)$, with a value of $C = n\mu_B^2 p^2 / 12\pi k_B$ corresponding to a derived magnetic moment $p = 9.5$, slightly larger than deduced from magnetic measurements,⁸ (ii) the derived Gd spin relaxation time plotted in Fig. 4, and (iii) the complex electronic conductivity given by the derived value of σ_1 in Fig. 3 and a value of σ_2 assuming $\lambda(0) = 140$ nm. The excellent fit to the experimental data supports our theoretical model and also the use of the approximate expressions for the effective conductivities where we have assumed $\omega\tau_s > 1$. In particular, there appears to be no need to invoke any

additional effects, such as a modification of the electronic mean free path from the Gd spin fluctuations.

In summary we have presented extensive microwave surface impedance measurements on GBCO single crystals at several frequencies to investigate the influence of the antiferromagnetic alignment of the Gd spin at low temperatures. We are able to describe the experimental results by a model involving the increase in magnetic susceptibility associated with antiferromagnetic alignment and a strongly temperature-dependent relaxation time. The derived spin lattice relaxation time increases below T_N with a temperature dependence $\sim T^{-5}$. Above T_N , $\tau_s \sim 1/(T - T_N)$. Within the accuracy of our measurements, $\sigma_1(T)$ is not affected by the antiferromagnetic alignment of the Gd spins.

We thank G. Walsh and D. Brewster for valuable technical support. We also thank A. Porch and M. Hein for useful discussions. This research is supported by the EPSRC, UK.

¹P. H. Hor, R. L. Meng, Y. Q. Wang, L. Gao, Z. J. Huang, J. Bechtold, K. Forster, and C. W. Chu, Phys. Rev. Lett. **58**, 1891 (1987).

²B. D. Dunlap, M. Slaski, Z. Sungaila, D. G. Hinks, K. Zhang, C. Segre, S. K. Malik, and E. E. Alp, Phys. Rev. B **37**, 592 (1987).

³H. A. Mook, D. McK. Pual, B. C. Sales, L. A. Boater, and L. Cussen, Phys. Rev. B **38**, 12 008 (1988).

⁴J. R. Waldram (private communication).

⁵S. M. Anlage, Lucia Mercaldo, and Vladimir Talanov (private communication).

⁶J. J. Wingfield, Ph.D. thesis, The University of Birmingham (1999).

⁷J. J. Wingfield, J. R. Powell, C. E. Gough, and A. Porch, IEEE Trans. Appl. Supercond. **7**, 2009 (1997).

⁸J. R. Thompson, B. C. Sales, Y. C. Kim, S. T. Sekula, L. A. Boater, J. Brynestad, and D. K. Christen, Phys. Rev. B **37**, 9395

(1988).

⁹Ruixing Liang, D. A. Bonn, and W. N. Hardy, Physica C **304**, 105 (1998).

¹⁰A. Erb, E. Walker, and R. Flükiger, Physica C **245**, 9 (1996).

¹¹H. Srikanth, B. A. Willemsen, T. Jacobs, S. Sridhar, A. Erb, E. Walker, and R. Flükiger, Phys. Rev. B **55**, R14 733 (1997).

¹²S. F. Lee, D. C. Morgan, R. J. Ormeno, D. M. Broun, R. A. Doyle, J. R. Waldram, and K. Kadowaki, Phys. Rev. Lett. **77**, 735 (1996).

¹³D. A. Bonn, S. Kamal, Kuan Zhang, Ruixing Liang, D. J. Baar, E. Klein, and W. N. Hardy, Phys. Rev. B **50**, 4051 (1994).

¹⁴J. van den Berg, C. J. Vanderbeek, P. H. Kess, J. A. Mydosh, G. J. Nieuwenhuys, and L. J. Dejongh, Solid State Commun. **64**, 699 (1987).

¹⁵K. N. Yang, J. M. Ferreira, B. W. Lee, M. B. Maple, W.-H. Li, J. W. Lynn, and R. W. Erwin, Phys. Rev. B **40**, 10 963 (1989).